



# Research on in situ monitoring of selective laser melting: a state of the art review

Dongju Chen<sup>1,2</sup> · Peng Wang<sup>1,2</sup> · Ri Pan<sup>1,2</sup> · Chunqing Zha<sup>1,2</sup> · Jinwei Fan<sup>1,2</sup> · Shuai Kong<sup>1,2</sup> · Na Li<sup>1,2</sup> · Jia Li<sup>1,2</sup> · Zhiqiang Zeng<sup>1,2</sup>

Received: 2 April 2020 / Accepted: 26 November 2020 / Published online: 3 March 2021  
© The Author(s), under exclusive licence to Springer-Verlag London Ltd. part of Springer Nature 2021

## Abstract

As an additive manufacturing technology, selective laser melting (SLM) can form any complex metal parts, which has unparalleled advantages compared to traditional processing methods. However, there are still some problems such as accuracy and non-repeatability to overcome to apply SLM to production practice. The high-precision monitoring and degradation feedback technology of SLM equipment is the future development direction. The real-time monitoring machine can repair itself and avoid the tedious detection in the post-processing stage. The researchers mainly monitor the quality of the forming process by molten pool signal, temperature signal, sound signal, and scanning track. The forming process is monitored using coaxial detection or paraxial detection through a high-speed camera, pyrometer, and other equipment. This paper can provide theoretical support for the SLM intelligent monitoring field.

**Keywords** Selective laser melting · In situ monitoring · Coaxial detection · Paraxial detection · Intelligent detection technology

## 1 Introduction

Selective laser melting (SLM), similar to welding, is a kind of layered production technology, which uses layered stacking to produce complex metal parts. In the atmosphere of inert gas (usually nitrogen or argon), the laser system selectively melts the powder on the powder bed according to the predefined 3D data model. The powder bed is deposited to a certain height according to the preset layer thickness, and the metal powder is evenly spread on the substrate by the scraper. The deflection direction of the laser beam is controlled by the galvanometer and f- $\theta$  field mirror to reach any position in the forming area. The tools and fixtures are eliminated since the laser beam and metal powder are used as manufacturing tools, and the advantages of the short production cycle, high material utilization

rate, and low cost by using SLM [1]. In theory, SLM can form any complex part and realize personalized customized service. SLM molding parts can be widely used in medical, mold, aerospace, ship, automobile, and other fields [2]. The schematic diagram of SLM equipment is shown in Fig. 1.

After decades of development, SLM has made great progress and can meet the manufacturing of complex 3D parts in most commercial fields. However, the quality of the SLM parts is far from the commercial standard. SLM-manufactured metal parts are difficult to be applied in actual production without post-processing, especially in the medical and aerospace fields with challenging quality and certification requirements. One of the main standards is that the manufacturing accuracy and forming quality related to the size required by the final product are not up to the standard. The industrialization of SLM is hindered by process instability and non-repeatability. The lack of in situ monitoring and process quality assurance is one of the main obstacles for SLM to be widely used in the modern manufacturing industry [4, 5]. The phenomenon of multiphysics involved in SLM is related to the strong changes in heat and radiation transmission during laser melting. Due to the uncertainty in the heat transfer process, different modes of powder melting to solidification may occur even in a single layer [6]. The effective thermal conductivity of powder with the particle size of tens of microns is 5–10

✉ Dongju Chen  
djchen@bjut.edu.cn

<sup>1</sup> Mechanical Industry Key Laboratory of Heavy Machine Tool Digital Design and Testing, Faculty of Materials and Manufacturing, Beijing University of Technology, Beijing 100124, China

<sup>2</sup> Beijing Key Laboratory of Advanced Manufacturing Technology, Faculty of Materials and Manufacturing, Beijing University of Technology, Beijing 100124, China

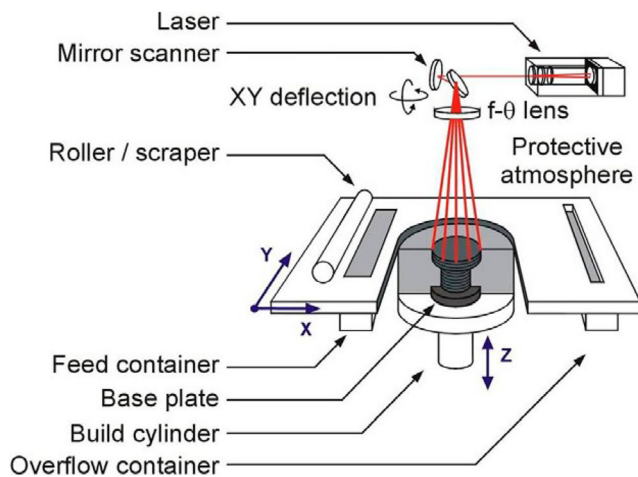


**Fig. 1** Schematic overview of the SLM machine (reproduced from [3], Copyright (2010), with permission from Elsevier)

times that of air, and its heat transfer becomes insignificant compared with the solidified specimen. The laser energy input easily leads to a high-temperature gradient because of the poor heat transfer effect of the powder. The high-temperature gradient produces thermal stress, which will cause deformation and even lead to molding failure [7].

There are many physical field phenomena in the SLM forming process, such as gravity, buoyancy, surface tension, capillary action, and the Marangoni effect. These phenomena will have different effects due to different materials and forming processes. More than 50 parameters affect the final quality of SLM due to the unique molding process (solid-liquid-solid), different powders, and process parameters [8]. These parameters can be divided into four categories: (1) process parameters, (2) powder material properties, (3) powder bed properties and recoding parameters, (4) molding environment parameters [9]. Most of them are predefined parameters, and only a few of them are adjustable (adjustable parameters include laser power, scanning speed, scanning hatch space, spot diameter, layer thickness, scanning strategy, exposure time, substrate preheating temperature, oxygen content, pressure, and other parameters). The SLM molding process is prone to produce internal defects due to many factors, but the post-processing of defects is very difficult or even impossible. Small changes in process conditions can lead to huge differences in microstructure [10]. The defects and errors in SLM can be divided into the following categories: (1) defects caused by equipment, (2) defects caused by process, (3) defects caused by model (or additive selection design), (4) defects caused by powder [11].

The cross-scale forming process of SLM should be studied using very precise time and space scales. From the micro-level, the powder is melted by laser to form a molten pool, and the stability of the molten pool directly determines the quality and stability of the forming process [12]. Adjust the process parameters in time to ensure the stability of the molten

pool according to the relevant information of the molten pool (including the width or area of the molten pool). The molten pool monitoring system can measure the temperature inside and around the molten pool, which is usually used for the development and comparison of multi-physical simulation. In addition to the monitoring of the molten pool, the change of the forming process caused by the change of process parameters also needs to be monitored and controlled. Spattering is one of the most common behaviors that lead to defects in the SLM forming process. The plasma produced by spattering is mainly divided into droplet spatter produced by liquid metal tearing and powder spatter formed when the non-molten metal powder particles around the molten pool are blown away [13]. Plasma can be monitored by in situ induction, including the amount of ejected material and the overall spattering behavior [14]. Besides, it is necessary to monitor the effect of the melting track and overlap to ensure the stability of the forming process. Defects such as internal pores of components are related to insufficient fusion and local overheating of the melting track. Monitor the shape, thickness, and temperature of the melting track to characterize the overall molding quality. Compared with the three-dimensional model, the accuracy of the molding process can be measured, and the existence of internal defects can be determined [15]. Therefore, the in situ quality control system should monitor and control the whole forming process, including the gas atmosphere, molten pool status, track shape, and temperature range.

SLM currently does not support in situ closed-loop control. It is an important way to support the development of SLM to monitor and control in situ by acoustic signal, optical signal, thermal signal, and other signals. The current research is only focused on the monitoring field, not the control field. But, monitoring is the precondition of control, and the excellent monitoring field can lay the foundation for the realization of closed-loop control in the future. The ultimate goal of SLM process monitoring is to effectively control the forming process with real-time closed-loop feedback [16]. Carrying out process-oriented real-time monitoring and feedback research and correcting or repairing when building components are the keys to ensuring high-quality SLM molding. For real-time monitoring, the optical sensor, acoustic sensor, temperature sensor, and other sensors are needed. The feedback circuit adjusts the process parameters in real time according to the signal collected by the sensor to obtain the required performance. The current research focuses on high-speed camera monitoring based on machine vision, sound monitoring based on sound wave, temperature monitoring based on molten pool thermal imaging, and component monitoring. It mainly monitors the information related to the molten pool, including the temperature, shape, area, spatters information, and element evaporation. The dynamic relationship between the acquired signal and process parameters is confirmed by system identification, and then, a stable robust controller is designed to

realize real-time feedback control. The ultimate goal of process monitoring is to ensure the forming quality of parts and reduce the dependence on expensive and time-consuming post-process inspection. With fast response time and high-resolution sensor, the variables and signals which are easy to analyze in the forming process are monitored, and the collected information is managed and analyzed to make decisions.

For the monitoring research of laser wire-based directed energy deposition (DED) processes, some documents give a better explanation [17, 18]. There are many kinds of research on visual monitoring [19] and temperature monitoring [20] of electron beam melting (EBM) technology in the current research, and monitoring equipment can be easily integrated into the equipment of electron beam melting processes. The accuracy and quality of SLM are higher than DED and EBM, and the forming process is accompanied by sound, light, electricity, and heat conduction that are difficult to monitor. The detection types include non-contact temperature measurement (pyrometer and infrared imaging), machine vision imaging, and low-coherence interferometry. Based on the sensor installation strategy, it can be divided into coaxial system and paraxial system. In the coaxial system, the monitoring sensor is placed in the laser path, and in the paraxial system, the monitoring sensor is placed outside the laser path. Compared with coaxial monitoring, paraxial monitoring can monitor the forming process without changing the machine equipment. The monitoring information provides detailed information on various phenomena in the molten pool and forming process with high-temporal and spatial resolution, which provides direct support for process optimization. It can be concluded that closed-loop control can ensure the stability of the forming process by monitoring relevant information and combining relevant data processing methods to develop optimization algorithms based on machine learning.

## 2 Coaxial detection

### 2.1 Cameras and pyrometers for monitoring

The preliminary research combines the optical measuring device based on temperature distribution in the sintering area by the camera with the online optical temperature monitoring system based on the highest surface temperature of irradiation point by the high-speed dual-wavelength pyrometer, as shown in Fig. 2. The thermal radiation intensity of the surface of the laser action area is recorded by a CCD camera or pyrometer at one or two spectral intervals and is related to the thermal radiation intensity of the blackbody simulator located in the same surface area. The system integrates two types of sensors: two-dimensional sensor digital CCD camera and single-point sensor pyrometer based on the photodiode. In situ temperature monitoring provides the possibility to optimize the forming process of high-porosity powder [21].

To continuously monitor the surface temperature (the temperature of the laser impact zone), Pavlov et al. used optical fiber to connect the dual-range pyrometer (11, Fig. 3a) recording the surface thermal radiation with the Phenix PM-100 optical unit (10, Fig. 3a). The results showed that the pyrometer signal generated in the laser impact zone is sensitive to the changes of the main operating parameters (powder layer thickness, hatch spacing, scanning speed, etc.), and the device can be used for in situ monitoring of molding quality. The influence of molding parameters on the structure and porosity can be judged by the different signals generated by the pyrometer [22]. To ensure that the intensity of LED scattering radiation exceeds all other emissivities except the laser impact area, an LED ring illumination system is used to illuminate the forming area [23]. Doublenskaia et al. added a CCD camera (560 × 760 pixels) to the device as shown in Fig. 3b. The CCD

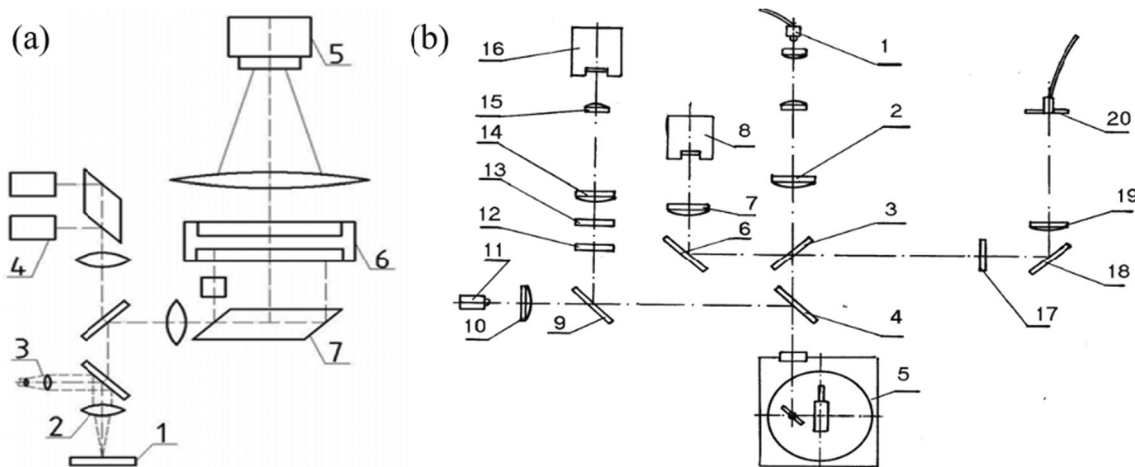
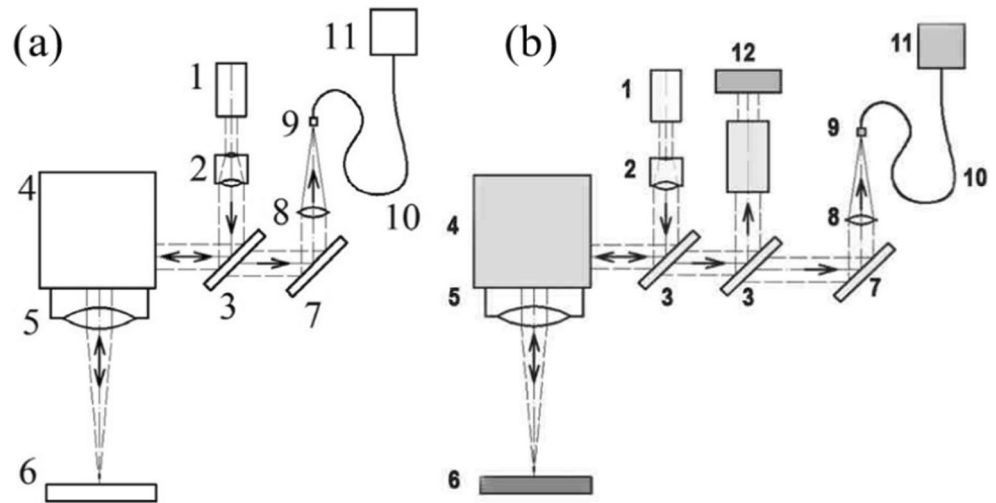


**Fig. 2** **a** Optical scheme of the system for temperature monitoring of the SLS machine: 1, working area; 2, focusing objective; 3, laser telescope; 4, photodiodes; 5, digital video camera; 6, MCP; 7, prism with dichroic coatings. **b** Monitoring system for the melting process: 1, fiber laser

output; 2, telescope; 3, 4, gradient dichroic beam splitters; 5, scanner head; 6, 9, 18, dichroic beam splitters; 7, 10, 14, 15, 19, lenses; 12, 13, 17, filters; 8, 16, CCD camera; 11, LED; 20, pyrometer fiber (reproduced from [21], Copyright (2010), with permission from Elsevier)

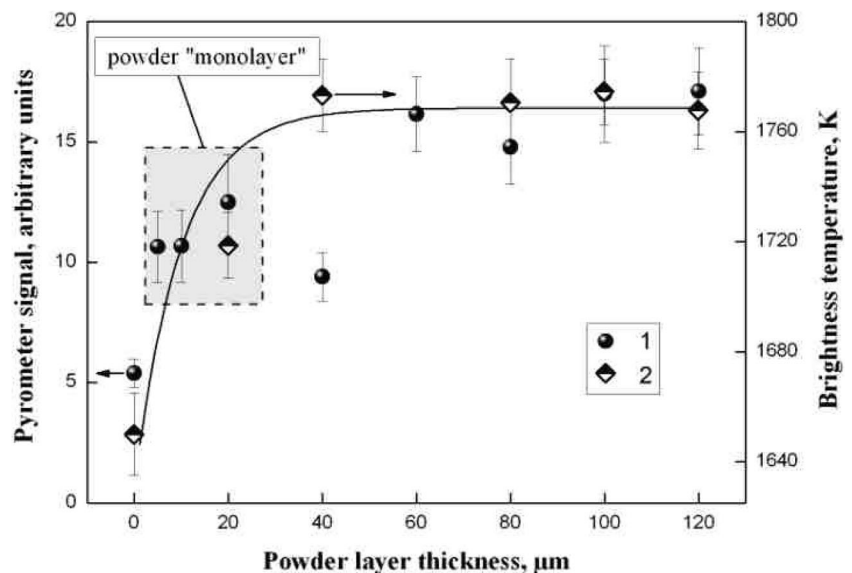
**Fig. 3** **a** Monitoring device with integrated pyrometer. **b** Monitoring device with integrated pyrometer and CCD camera. 1, fiber laser; 2, beam expander; 3, laser beam/thermal signal separating mirror; 4, scanner head; 5, F-theta lens; 6, powder bed; 7, mirror; 8, pyrometer lens; 9, fiber tip; 10, optical fiber; 11, pyrometer; 12, CCD camera (reproduced from [22, 24]. Copyright (2010,2012), with permission from Elsevier and Japan Laser Processing Society)



camera (12, Fig. 3b) measures the thermal radiation from the heat-affected zone (HAZ). Because the coefficient of thermal conductivity of the powder bed is 20 times lower than that of bulk material, the average temperature increases with the increase of powder layer thickness. From a certain critical value, the pyrometer signal and brightness temperature reach the maximum value and stable value due to the disappearance of the contact between the melted powder layer and the substrate. Therefore, all laser energy is absorbed by the powder and there is no heat loss in the substrate (as shown in Fig. 4). Berumen et al. [25] used a coaxial monitoring system to monitor the active construction area and allowed a resolution of 10  $\mu\text{m}$  per pixel. The results showed that the temperature gradient of the whole construction area can be identified by the photodiode sensor.

Molten pool monitoring equipment can be used to monitor the molten pool because the wavelength of the laser beam is different from that produced by the molten pool. Craeghs and Clijsters designed a coaxial monitoring system, as shown in Fig. 5. The laser source is deflected to the F- $\theta$  field mirror through the half mirror, and the F- $\theta$  field mirror focuses the laser beam on the working area to melt the powder. The powder melts to form a molten pool, and the radiation generated by the molten pool is transmitted to the beam splitter through the F- $\theta$  field mirror and the semi-mirror. The radiation separated by the beam splitter is transmitted to the planar photodiode and high-speed CMOS camera. Planar photodiodes capture laser radiation in a certain range of wavelengths, and high-speed CMOS cameras are responsible for collecting pool characteristics such as melt area, length, and width. The upper

**Fig. 4** Variation of the pyrometer signal and variation of the maximum brightness temperature in HAZ measured by CCD camera with a powder layer thickness (reproduced from [24] with permission from Japan Laser Processing Society)



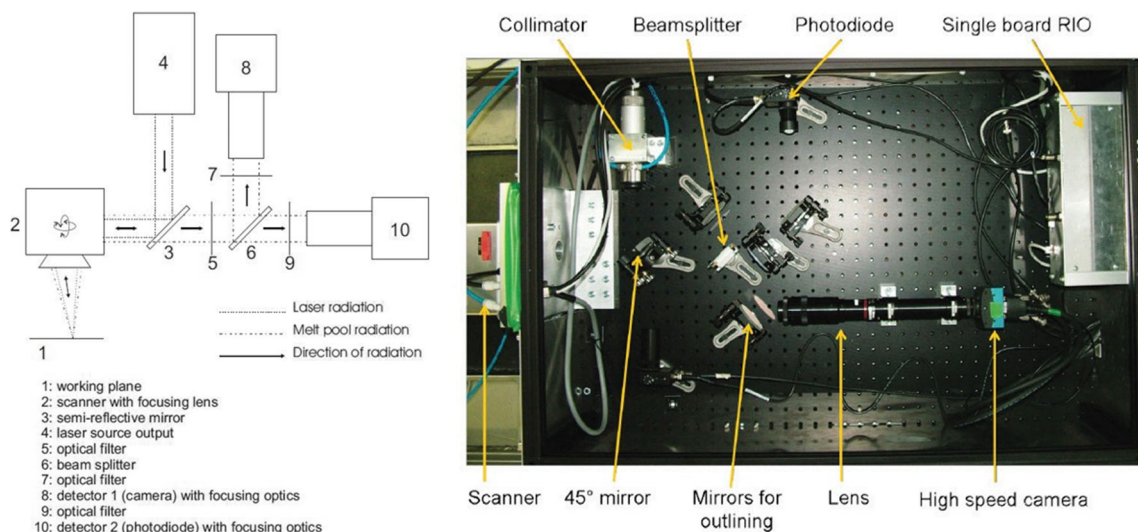


**Fig. 5** Schematic overview of the experimental setup to the monitoring system (Reproduced from [3, 28], Copyright (2010,2012), with permission from Elsevier)

limit of the captured wavelength is set to 950 nm to avoid laser induction (laser wavelength is 1064 nm), and the 780-nm wavelength higher than the visible light threshold is set as the lower limit. The system can distinguish the area of molten powder and air hole and realize the real-time processing of the molten pool image by using a field programmable gate array cell. The results show that actual defects (after cutting specimens or using X-ray CT scans) have good compatibility with defects observed in situ by the coaxial monitoring system [3, 26]. The 3D reconstruction defect detected by the system is almost the same as that detected by X-ray computed tomography. Furthermore, they studied the response of the system in dealing with different part geometry [27] and developed the technology of mapping the molten pool data to the plane coordinate system [28].

The temperature gradient of SLM determines the microstructure and mechanical properties of the parts. The proper temperature gradient can form high-quality specimens, and the poor temperature gradient distribution will lead to the powder not melting (too low temperature) or element evaporation (too high temperature). Therefore, it is necessary to monitor the temperature during the forming process. Yadroitsev et al. used a CCD camera coaxial optical detection system equipped with a resolution of  $782 \times 582$  pixels to collect signals to monitor the temperature distribution in the molten pool, as shown in Fig. 6 [29]. To measure the brightness and temperature of the laser-irradiated area, the monitoring equipment projects the molten pool image with five times magnification onto the CCD camera. With the increase of laser power and exposure time, the maximum temperature of the molten pool increases significantly. To visualize the dynamics of the molten pool, Lott et al. added an illuminating

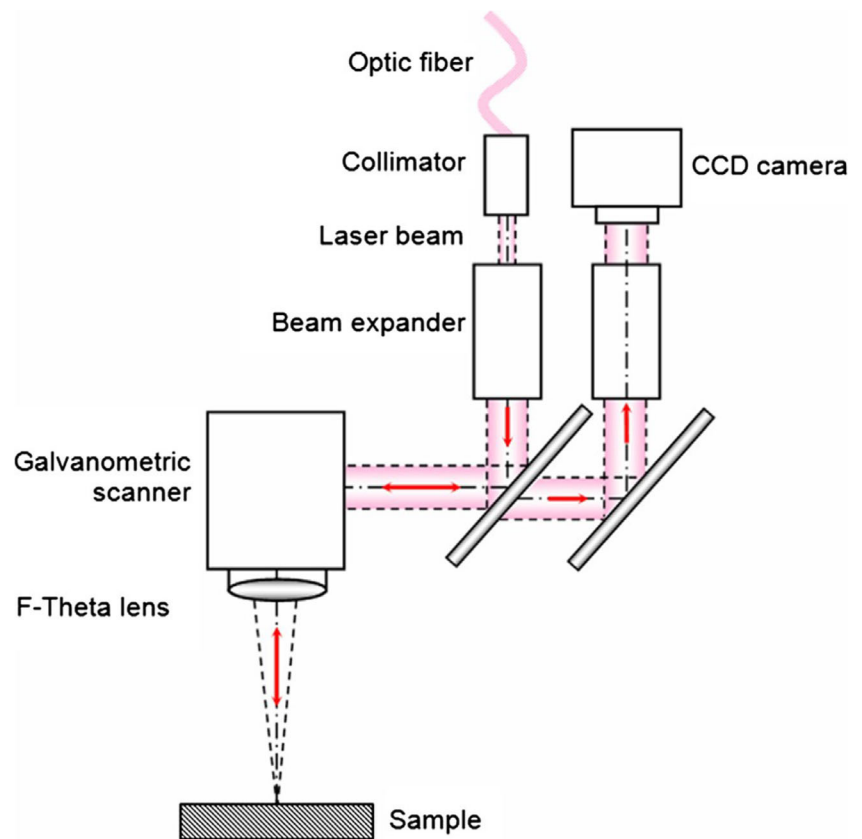
laser beam (with a different wavelength from the intense laser used for melting) during the forming process. The radiation intensity of the molten pool will be higher when the illumination laser is added, so the camera can capture images at a high sampling rate to enhance the visualization of the dynamics of the molten pool. However, with the addition of the illumination laser, the temperature measurement cannot be carried out because the incandescent radiation from the processing area is smaller than that from the reflected illumination [30, 31].

## 2.2 In situ coherent diffractive imaging for monitoring

The study of powder-related state can reveal the key topological information closely related to the final part quality. Low-coherence interference imaging (in-line coherence imaging, ICI) technology is used in the SLM process, which is robust to deal with the interference of laser and radiation. ICI is a low-coherence interference imaging technique closely related to spectral-domain optical coherence tomography (SD-OCT) [32]. ICI can allow high-speed microscale morphology measurement, which can identify the physical state of the specimen (i.e., the relationship between powder, melt, and solidification track) and the characteristics of unstable melt formation caused by defects [33].

Neef et al. integrated sensors into SLM production units based on ICI [34]. To overcome the limitation of static interface monitoring, Jordan has developed a device based on ICI to monitor the pool dynamics, as shown in Fig. 7. The system consists of a low-power broadband light source, a high-speed spectrometer, and an optical fiber Michelson interferometer (Fig. 7a). Fiber-coupled broadband light emitted by SLD first passes through the optical isolator to prevent reflection. A

**Fig. 6** The optical system for temperature measurements (reproduced from [29], Copyright (2014), with permission from Elsevier)



50:50 beam splitter is used to split the light into the sample arm and the reference arm. The light in the sample arm is coaxially combined with the processing laser beam through a dichroic mirror. Figure 7b–c shows the in-line coherent imaging monitoring systems integrated into two different selective laser melting systems. A common laser processing objective is used to focus the combined beam on the sample. The imaging light is backscattered from the specimen and collected by the sample arm optical fiber. The light in the reference arm passes through the fiber polarization controller and the dispersion matching element to compensate for the polarization change caused by the single-mode fiber and the

dispersion caused by the optical element in the sample arm. The light in the reference arm is reflected from the reflector and coupled to the interferometer. The reflected light from the sample arm and the reference arm is reflected by the beam splitter and transmitted to the spectrometer. The relative optical path difference between the sample arm and the reference arm results in the electric field phase difference, which leads to the combined intensity spectrum (i.e., interferogram). SD-OCT interpolation, Fourier transform technology, or single-step homodyne filtering technique can be used to process the collected signals. ICI technology is suitable for measuring the pool strength, height, and longitudinal size along the

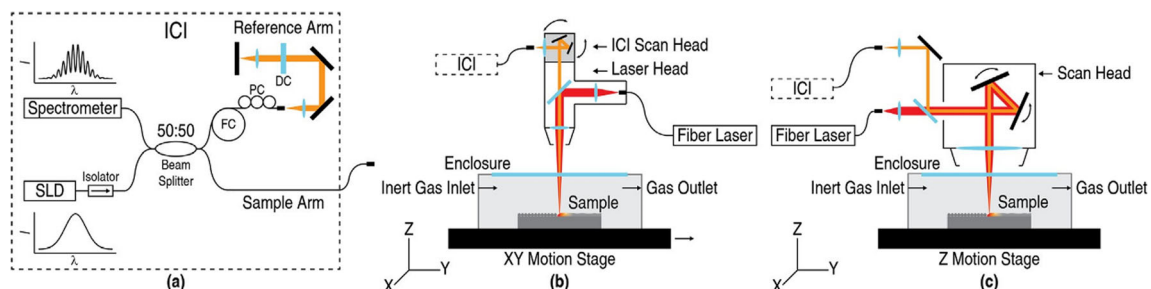


**Fig. 7** The system of laser imaging processing. **a** The ICI system: SLD, superluminescent diode (SLD); FC, coiled fiber; PC, polarization controller; DC, dispersion compensating elements. **b** The system of melting pool imaging for morphology measurements of the melt zone and surrounding

areas. **c** The system of laser processing control with coaxial imaging for faster processing speeds (reproduced from [33], Copyright (2016), with permission from Elsevier)

monorail, so that different types of defects can be detected, including spheroidization, lack of fusion, excessive melting, and other surface irregularities.

### 3 Paraxial detection

#### 3.1 High-speed camera for monitoring

In the coaxial monitoring system, the optical elements of the laser beam melting system need to be retrofitted. Also, all the monitoring systems cannot compare the monitoring results with the quality of the final molding, only limited to the current molten pool and its surrounding environment. The process error can be monitored without changing the equipment by using paraxial monitoring. Many scholars use the high-speed camera or infrared camera to monitor the forming quality. The high-speed vision system is used to monitor the melt state, while the low-speed but high spatial resolution camera monitors the state of the powder layer or when it forms a track. Due to the airtightness of the molding space, germanium or B270 ultra-white glass is needed to close the molding chamber [35].

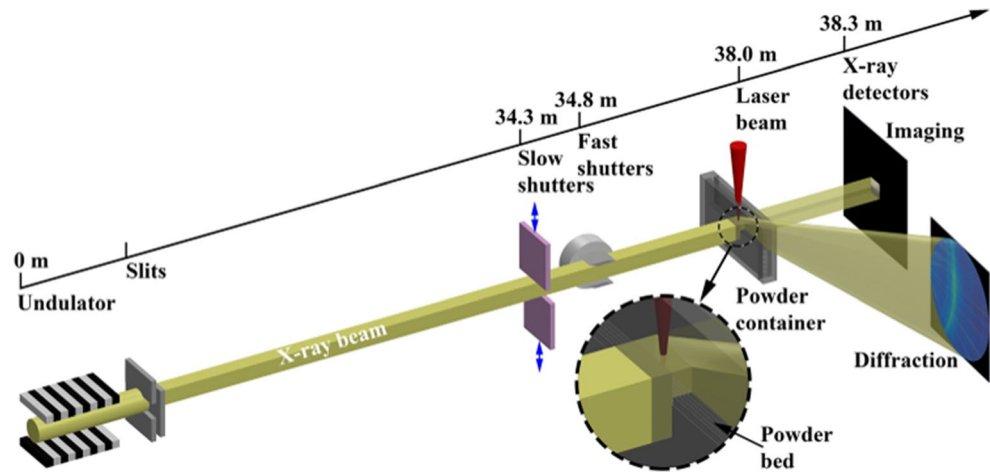
Kleszczynski et al. [36] used a monochromatic CCD camera system for visual detection and error analysis. The camera (SVCam-hr29050, SVS-VISTEK GmbH) was installed outside the window of the machine, and the image in the molding chamber is taken from the viewing angle. The tilt and shift lenses (Hartbli Macro 4/120 TS Superrotator) help reduce perspective distortion by moving the camera backward. The camera uses a  $36 \times 24$ -mm Kodak 29 megapixel sensor (6576 by 4384 pixels, pixel size  $5.5 \mu\text{m}$  by  $5.5 \mu\text{m}$ ). The structure used to provide uniform illumination for the metal weld is added to minimize the mirror reflection that will saturate the camera CCD sensor to ensure the best imaging quality. It is found that diffuse illumination can produce the best surface image quality when the light source is close to the working surface and back to the camera.

The imaging system can measure geometric features, so it can be used to control the size accuracy. Jacobsmühlen et al. used the system to detect the surface quality and defects of specimens, and the results can be used for process optimization [37]. When it is detected that the layer is not completely covered by powder, the salient point can be captured. With the increase of laser power, the outer region increases, which makes the powder layer unable to cover the rising region. These areas are detected and highlighted by a white box (bottom). Reducing the laser power can effectively improve the forming quality. Reducing the hatch space will lead to higher energy input, resulting in a poor molding effect and more white boxes. Then, they developed image analysis and processing software to identify the lifting area of the whole powder bed. The

quantitative measurement method is used to analyze all construction layers of the construction areas and parts. To speed up the identification process and reduce the amount of calculation, the powder layer image acquisition and imaging system were used to evaluate the processing behavior of the supporting transition and overhanging structure by measuring the total area of the rising area and the average area of the connected area [38]. The team monitored the bulge area in the molding process, comparing the high-resolution image after powder deposition with the high-resolution image after melting. By comparing the high-resolution image after powder deposition and the high-resolution image after melting, using a stochastic gradient descent classifier and a stereo matching problem descriptor with an angular resolution of  $A = 20^\circ$ , the cross-validated F1-score (for the definition of F1-score, please refer to the original literature.) can be reached 0.67 [39].

Hirvimäki et al. used a spectrometer to measure the spectral content of the molten pool radiation, a pyrometer to measure the temperature change of the molten pool, and a CCD camera for active lighting. The visual information of the molten pool in the process of processing under different scanning speeds, layer thickness, and hatch spacing is obtained by using this method [40]. Zhao et al. used high-speed X-ray imaging and diffraction (as shown in Fig. 8) to monitor the process of laser powder bed fusion. As shown in Fig. 9a, it can be observed that the process starts with the melting of the Ti-6Al-4V powders around the laser spot and then the Ti-6Al-4V base. A small cavity or depression area is formed as the powder moves inside and outside the powder bed. A dome-shape metal structure without obvious structural defects is formed in the end. As shown in Fig. 9b, the interaction between laser and metal is much more violent than that in Fig. 9a. The balance of surface tension and recoil pressure also governs the melting process shown in Fig. 9a, but in the case shown in Fig. 9b, their combined effects on the melt pool dynamics and powder motion are much higher [41]. The high-speed camera can be used not only to monitor the molten pool but also to monitor the powder spreading state and the forming continuity. Craeghs et al. [42] constructed a monitoring platform using a visual camera with a focus lens and three light sources. Two types of defects caused by scraper are detected by the way of front lighting: one is that the abrasion of the scraper will cause a small scratch in the whole area and the other is that local damage of scraper will cause a local deep scratch. He also developed a system to monitor the status of the molten pool. Through the monitoring of the molten pool area and the length-width ratio of the molten pool, the input parameters (laser power and scanning speed) of the molten pool can be real-time feedback controlled. Due to the dynamic of the SLM process, the processing rate of real-time feedback control based on the high-speed camera must be at least about 10 kHz.

**Fig. 8** Schematic of the high-speed X-ray imaging and diffraction experiments on laser powder bed fusion process at the 32-ID-B beamline of the Advanced Photon Source (reproduced from [41], Copyright (2017), Open access)



Krauss et al. used a long-wave infrared (8–15  $\mu\text{m}$ ) camera which was limited to 50 frames per second, and the time constant of the sensor was 5–15 ms. Although the location and size of the weld pool cannot be distinguished, defect detection can still be carried out [38]. Bayle et al. used a mid-infrared (3–5  $\mu\text{m}$ ) camera to capture the thermal image of the SLM forming process area, and quantified the size and

splashing speed of plasma [43]. As shown in Fig. 10, Repossini et al. used a high-speed machine vision system to study the impact of spatter on the molding quality. The high-speed camera captures images at a rate of 1000 frames per second to capture the splashing behavior at a sufficient time resolution. The results showed that splashing behavior can be used to characterize the process stability. Identifying different

**Fig. 9** Dynamic X-ray images of laser powder bed fusion processes of Ti-6Al-4V. The laser powers are 340 W for image group (a) and 520 W for group (b), respectively (reproduced from [41], Copyright (2017), Open access)

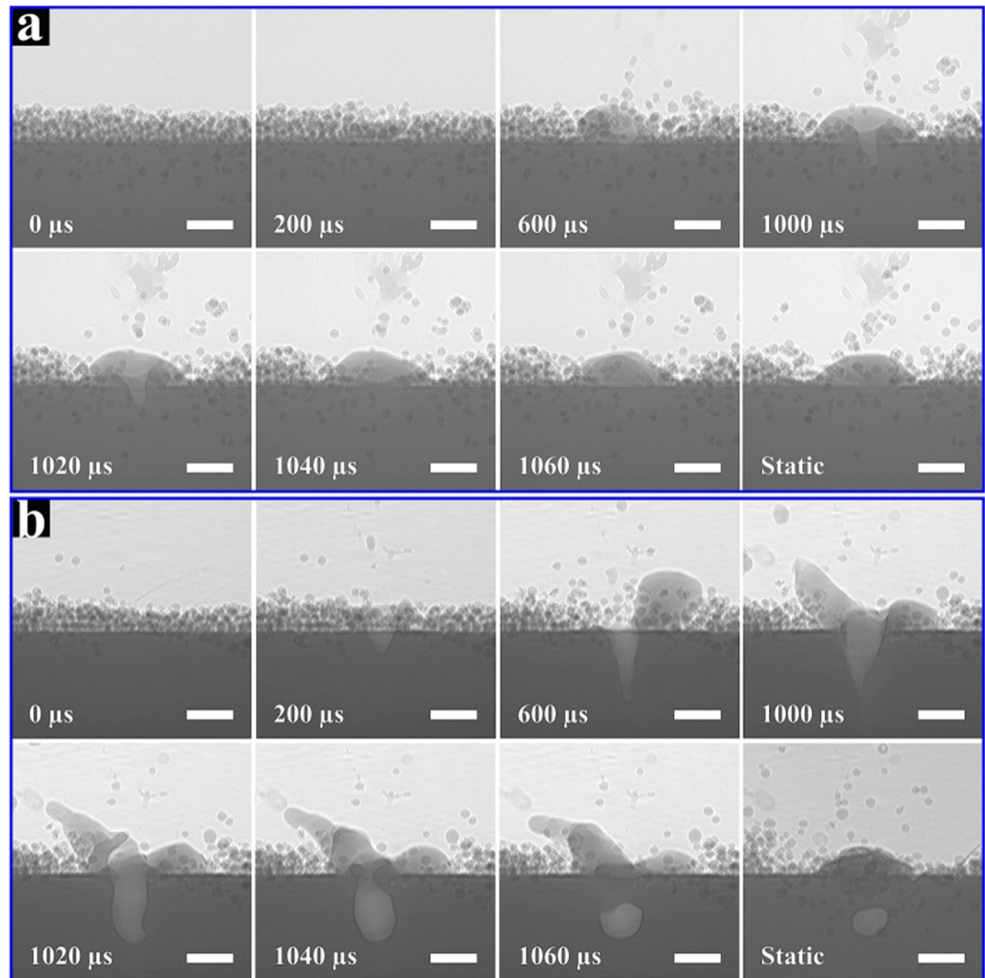
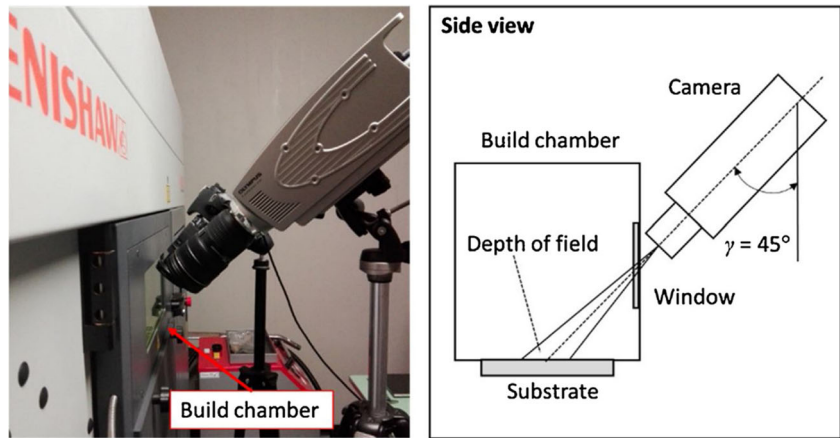




**Fig. 10** Off-axial mounting of the high-speed camera outside the build chamber (reproduced from [44], Copyright (2017), with permission from Elsevier)



patterns of the spattering behaviour to classify the current melting state through the research and modeling of splash behavior [44], as shown in Fig. 11.

Furumoto et al. [45] monitored the melting process and solidification process of metal powder by a high-speed camera (recording speed of the high-speed video camera was 10,000 fps). The results showed that when the metal powder is heated to form a melting zone, the laser irradiation zone scatters circumferentially. The shape of the solidified structure is affected not only by the surface tension caused by the melting of the metal powder but also by the adhesion caused by the wettability. Islam et al. [46] used a Baumer CMOS camera with

Cavitar CAVILUX diode laser illumination to monitor the spheroidization during the molding process. The balling was reduced by increasing the energy input. When the energy input exceeds a certain value, the balling was visible again. The research of Kruth et al. [47] found that the combination of high laser power and high scanning speed can reduce the occurrence of spheroidization. Ciales et al. [14] used real-time thermal imaging device to collect the melt and surrounding temperature. It is possible to infer changes in the sizes of melt pools from the thermal camera recording by observing the size of the measurable isotherms surrounding the actual liquidmelt pool. The result of image segmentation using liqui dus temperature as

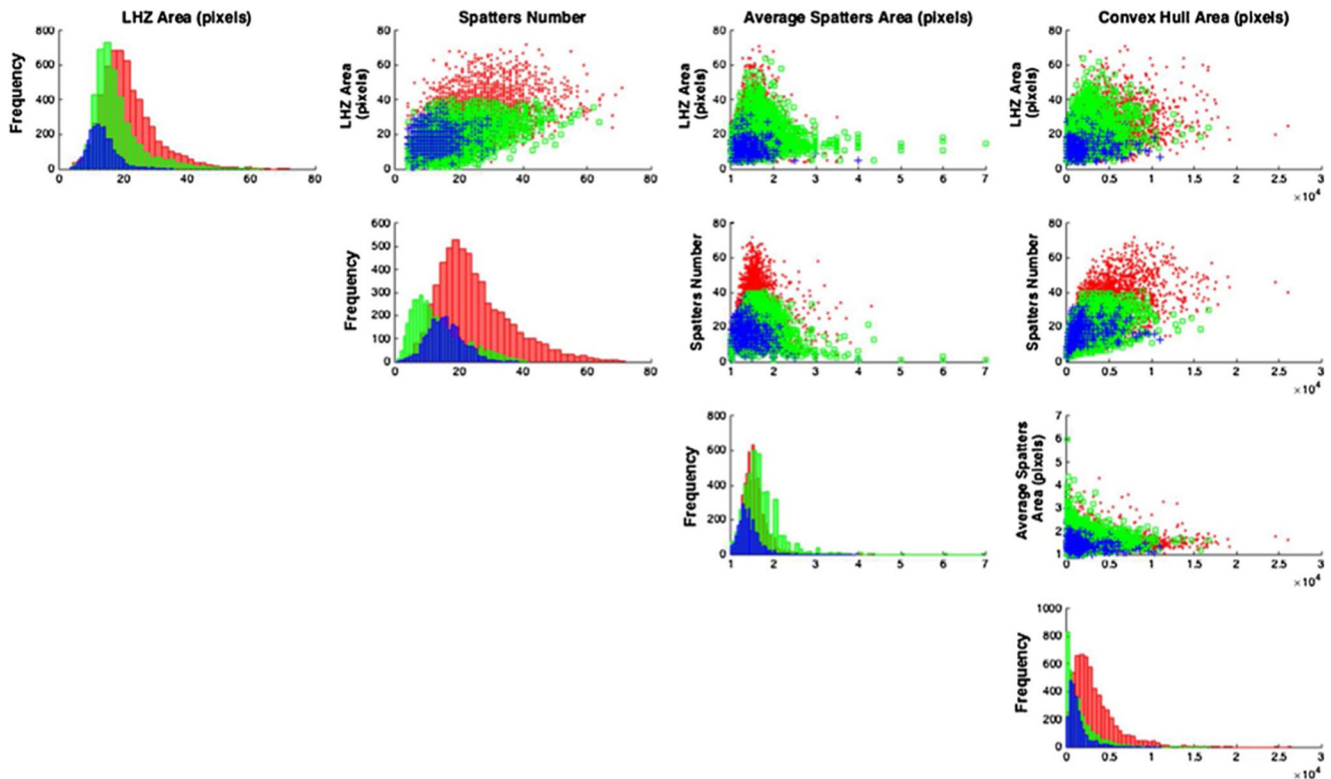


**Fig. 11** Scatterplot of spatter and the laser heated zone (LHZ) descriptors; blue crosses: under-melted, green squares: normal-melted, red circles: over-melted (Reproduced from [44], Copyright (2017), with permission from Elsevier)

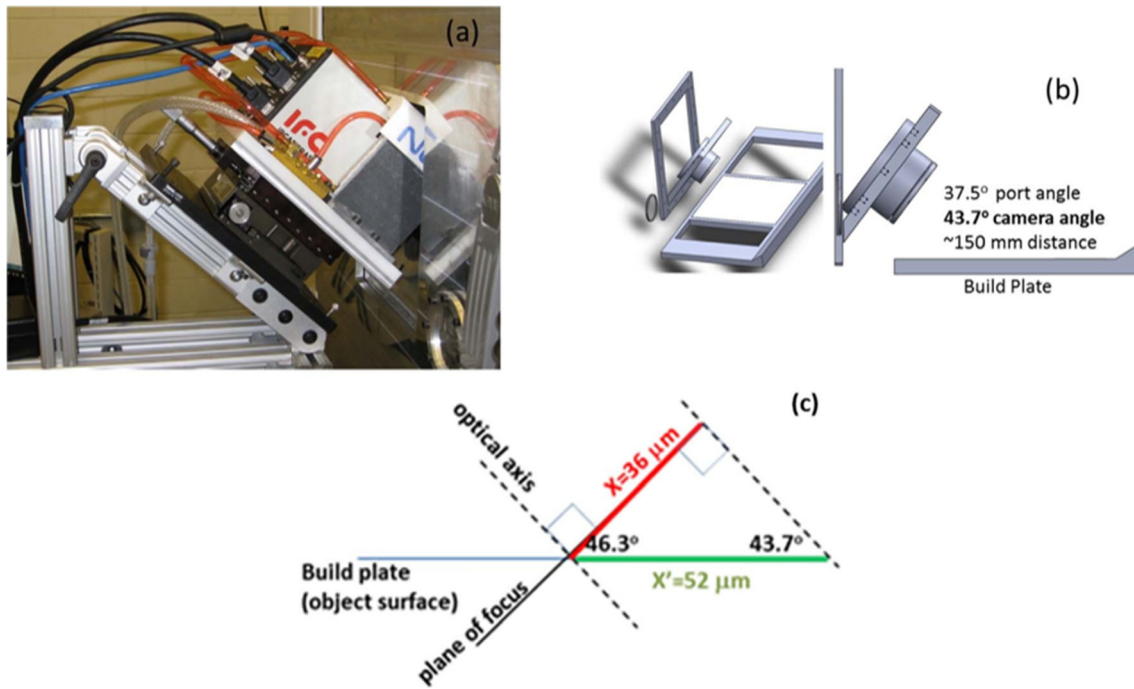


**Fig. 12** Thermal camera setup. **a** Side view of the laser powder bed fusion (L-PBF) machine, custom door, and thermal camera. **b** CAD solid model of L-PBF machine build chamber and custom viewport. **c** Optical

axis, plane of focus, and vertical iFoV projected on the build plane (reproduced from [14], copyright (2017), with permission from Elsevier)

threshold on single frame is shown in Fig. 12, where the molten region is marked red and the cooler region is marked blue.

Krauss et al. [35] established a low-cost radiometer camera for process monitoring and studied its sensitivity to process deviation detection. The camera has a long-wave infrared range (LWIR) and a sampling rate of 50 Hz. The device can identify the deviation caused by process parameter drift or random process error during the molding process and detect the inner cavity and defect at the same time. However, the monitoring range of the equipment is 160–120 mm, which accounts for about 30% of the total forming area. To find out the correlation between the temperature distribution, the stability of the forming process, and the final product quality, Krauss et al. studied the influence of scanning vector length, laser power, and layer thickness and distance between parts on the thermal distribution of specimen [48]. The key indicators are assigned to every position of the current cross section of the entire layer, as shown in Fig. 13. A three dimensional quality report for key indicators can be generated through

stacking of individual layer data. Monitoring and evaluation of solidification and layered deposition can help identify defects in the early stages of the solidification process.

Krauss used thermal imaging equipment to monitor the changes in thermal history caused by parameter changes [49], as shown in Fig. 14a. The camera uses a  $640 \times 480$ -pixel focal plane array and operates in the spectral range of 7 to 14  $\mu\text{m}$ . Combined with a 50-mm lens, it can achieve a resolution of about 250-mm pixels. Collect information about all layers of part quality by monitoring the information of each layer. The 3D quality report similar to the tomographic method is formed by deriving the quality index map of each layer (as shown in Fig. 14b–e). The device can well evaluate the thermal history of forming and associate with forming quality.

Abdelrahman et al. [50] described a device for monitoring fusion defects of powder bed by using optical imaging technology, as shown in Fig. 16. The system is equipped with a 36.3 megapixel DSLR camera (Nikon D800E) with an image size up to  $7360 \times 4912$  pixels. The device with multiple flash

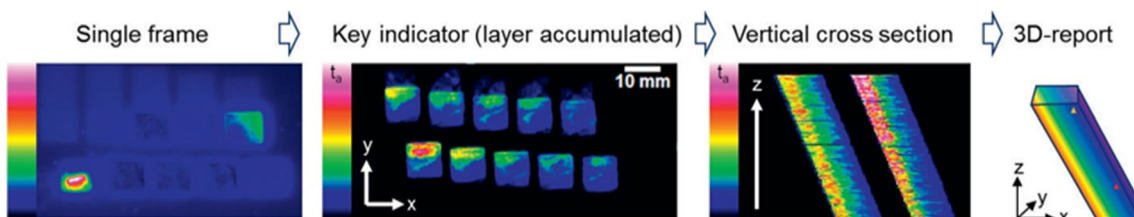


**Fig. 13** Data processing to generate a visual quality report (reproduced from [48], Copyright (2014), with permission from Elsevier)

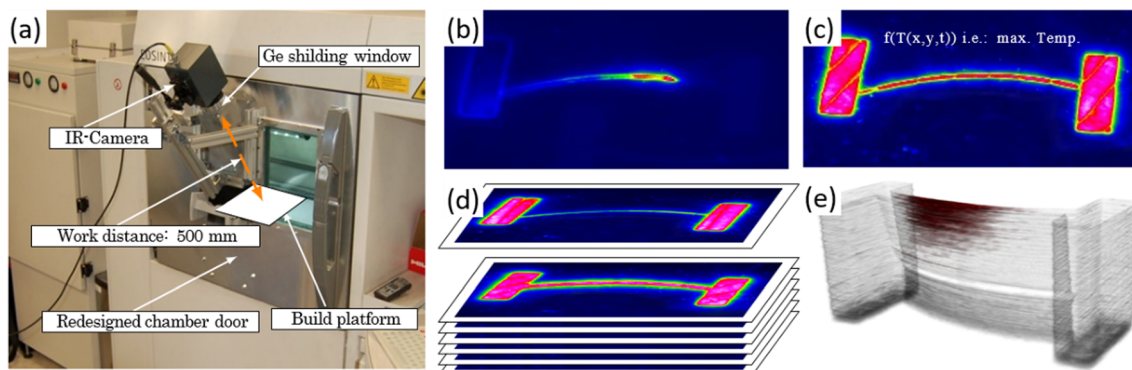


**Fig. 14** a Measurement setup. b live frame during the solidification process. c Accumulated key indicator. d Layer wise composition of key indicator. e 3D quality report (reproduced from [49], Copyright (2015), with permission from AIP Publishing)

modules is installed in the cabin of EOS M280, which can obtain images after powder scattering and laser exposure. Four photos are taken by flash 1–4 (the position of flash is shown in Fig. 15) after repainting, and one photo is taken when indoor lighting is turned on. The acquired image is segmented by the binary template. The intentional defects are designed into the parts at different positions, and then, the defects are detected automatically. The results showed that the accuracy is high.

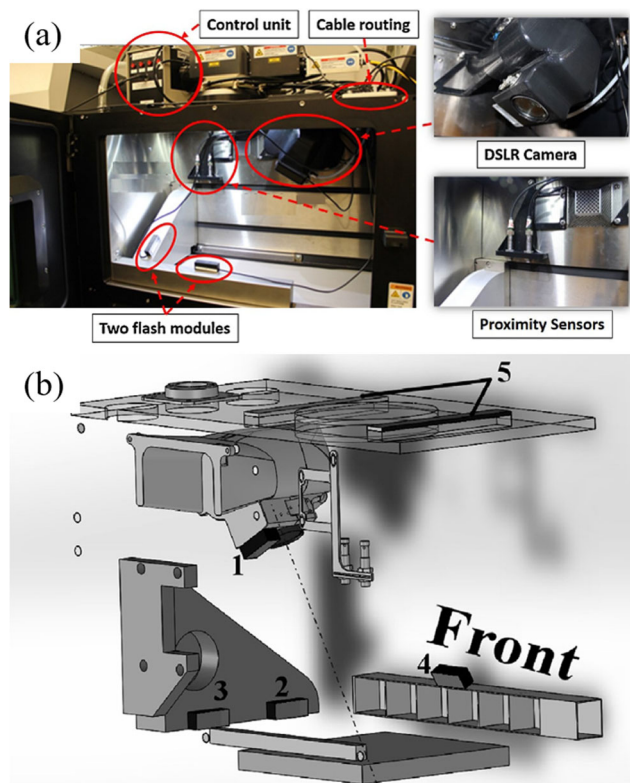


**Fig. 15** a The system of monitoring equipment. b 1–4, the location of flashes; 5, the location of chamber lights (reproduced from [50], Copyright (2017), with permission from Elsevier)

### 3.2 Sound collector for monitoring

The laser may be affected by the characteristics of the lens in the Lagrange coordinate system when using coaxial monitoring. The laser is easily affected by the angle and distance when using paraxial monitoring, even if the strong signal is received in the Eulerian reference frame. Acoustic sensors have many advantages in SLM process monitoring due to their non-contact, non-destructive and flexible nature, as shown in Fig. 16. Ye et al. [51] proved the feasibility of acoustic signal quality monitoring through experiments. The features of the collected signals are extracted, and then, defect detection is carried out using the directed belief network (DBN) framework. The formation of trajectory in the SLM forming process is related to the sound signal, and the sound signal is related to the change of splash particles. Therefore, the sound signal in the forming process of SLM can be used to predict the forming track of SLM.

### 4 Other in situ monitoring cases

Sigma Labs PrintRite3D is currently the most commonly used quality control method for additive manufacturing quality assurance and process monitoring. The computer automatically compares the similarities and differences between the captured images and the slices of the design model by processing the acquired digital image. The program instructions will stop the operation of the equipment when the gap is large, and the equipment will continue to operate when the gap is not obvious but will send a warning. The warning can be used as an inspection object in the quality inspection process after printing. Leung et al. [52] used high-speed synchronous X-ray imaging to monitor defects in laser additive manufacturing and weld pool dynamics. By operating the high-speed synchronous X-ray imaging, as shown in Fig. 17, the basic physical phenomena of the molten metal deposition orbit are revealed. Monitoring shows that laser-induced gas/steam jets



**Fig. 16** The system of acoustic signal acquisition (Schematic diagram)

promote the formation of melt traces and exposed areas. The pore migration mechanism of the flow driven by Marangoni was also found. X-ray imaging can be achieved with unprecedented time (a few tenths of a microsecond) and spatial resolution (a few microns) through a high-throughput X-ray beam from a synchrotron radiation source.

## 5 Intelligent detection technology

Intelligent monitoring technology mainly combines on-site detection and intelligent algorithms and uses machine learning or deep learning algorithms for image processing. The application of deep learning algorithms in the SLM field can control product defects (such as pores and cracks) and ensure product quality. The monitoring system using deep learning

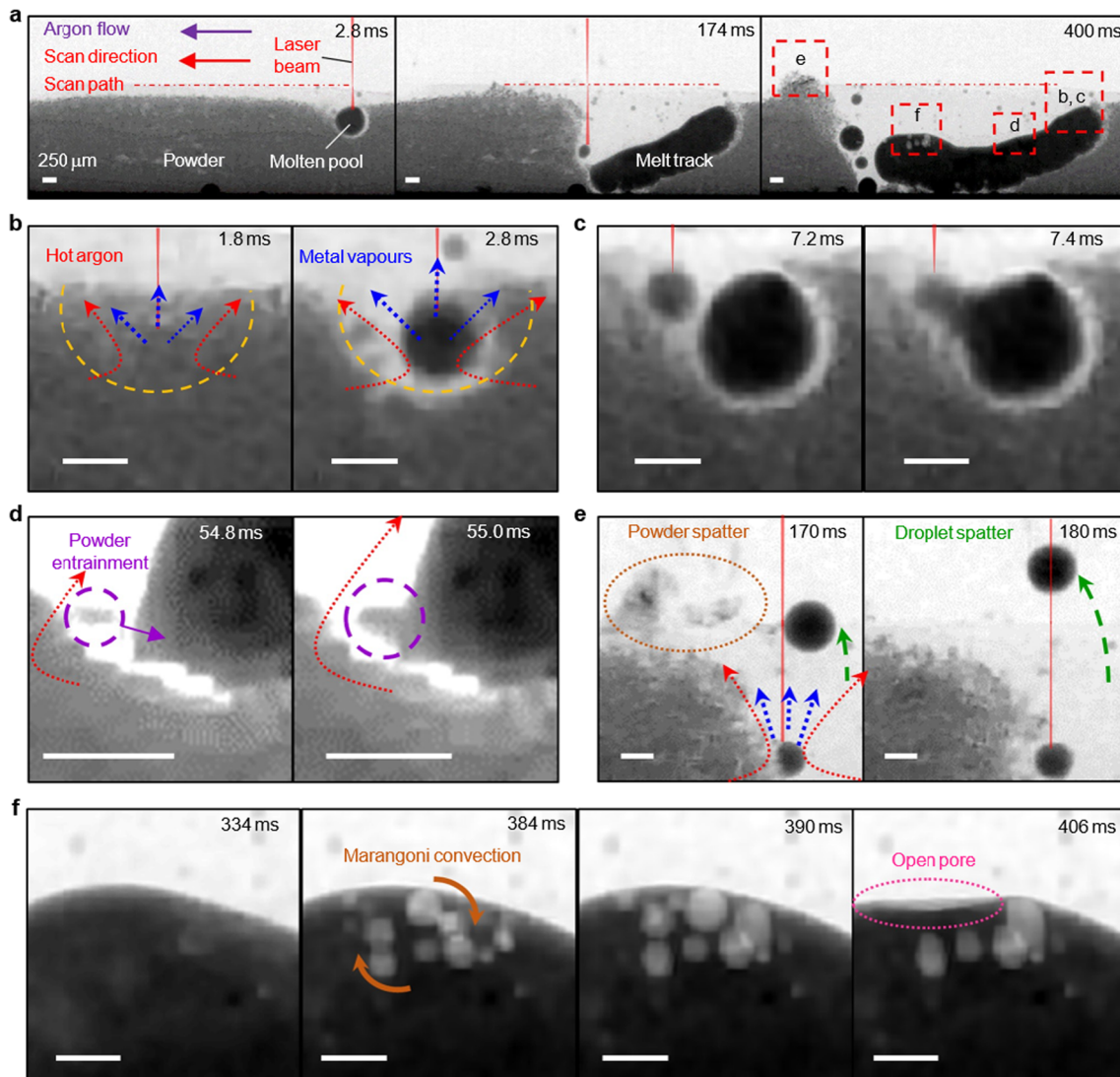


**Fig. 17** **a** The melt track morphology at three key stages of LAM. **b** The formation of a molten pool and a denuded zone (yellow dotted line). **c** Molten pool wetting. **d** Vapor-driven powder entrainment (orange dotted

semi ellipse). **e** Powder spatter (purple dotted circle). **f** Open-pore (pink dotted line). All scale bars = 250  $\mu\text{m}$  (reproduced from [52], Copyright (2018), Open access)

algorithms can monitor and control the parameters of the molding process online to achieve real-time feedback. Intelligent methods have been widely used in manufacturing process monitoring and defect detection. Neural network (NN) is the most studied method and has been used in detection scenarios such as welding defect identification [53]. Yuan et al. [54] used an image processing algorithm based on a convolutional neural network (CNN) to build the core framework of the online monitoring system of SLM. More than 1000 videos collected in the experiment are trained by CNN to identify the required quality indicators. It has been proved that the algorithm can be applied in the process of processing with high application reliability. Scime et al. [55, 56] developed an algorithm based on machine learning and computer vision, as shown in Fig. 18, which can be well used as a post-build analysis tool to enable the user to identify fault patterns and locate areas in the final part that may contain macroscopic (millimeter) defects.

The plasma produced in the forming process includes the ionized gas from the atmosphere and the evaporated or ionized metal from the powder bed. The plasma may absorb or refract the laser radiation, thus affecting the energy absorption of the melt [57]. The thermal radiation from the molten pool is usually in the visible to an infrared range (900 to 2300 nm), while

the plasma emission wavelength is in the near ultraviolet or visible wavelength (400 to 650 nm), and the laser backward reflection occurs in the laser wavelength 1060 to 1080 nm [30]. Therefore, we can use different radiation wavelengths to monitor the plasma. Repsini et al. confirmed that plasma can be used as a feature for real-time adjustment of the SLM process [44]. As shown in Fig. 19, plasma is mainly caused by three sources, namely recoil pressure, the Marangoni effect, and the heating effect of the molten pool. Different sources lead to different splash patterns [58]. Grasso et al. [59] extracted plume features from infrared video and constructed an SLM molding zinc powder in situ monitoring system using K-chart, forming an evaluation system for judging processing quality. Yang et al. [60] proposed a maximum entropy dual-threshold image algorithm based on a genetic algorithm (MEDTIA-GA) to identify plasma. This method uses the maximum entropy segmentation algorithm as the fitness function. The genetic algorithm will automatically find the global threshold in a short time by maximizing the pixel information entropy. The results showed that the new image processing algorithm eliminates three types of segmentation errors (noise sensitivity, splash adhesion, and splash omission), as shown in Fig. 20. Compared with other algorithms, the MEDTIA-GA method gives the most accurate feature of the splash.

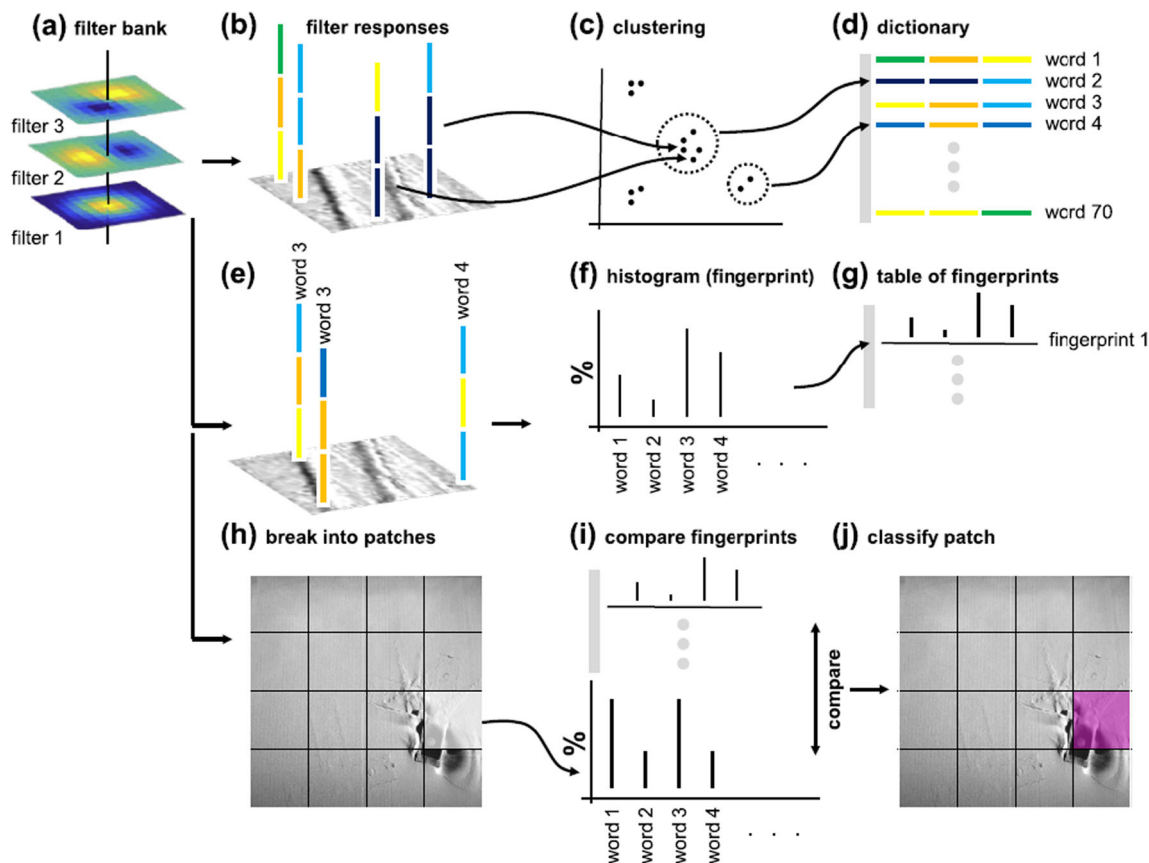
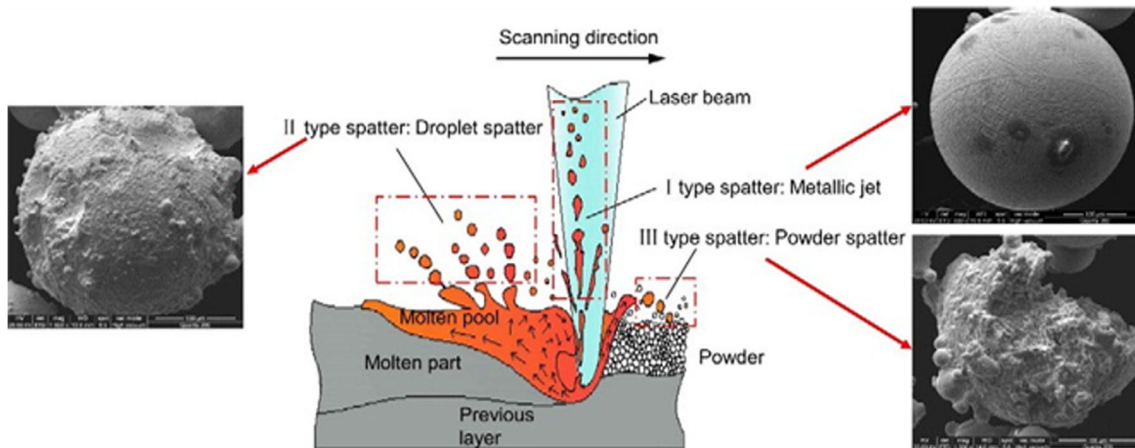
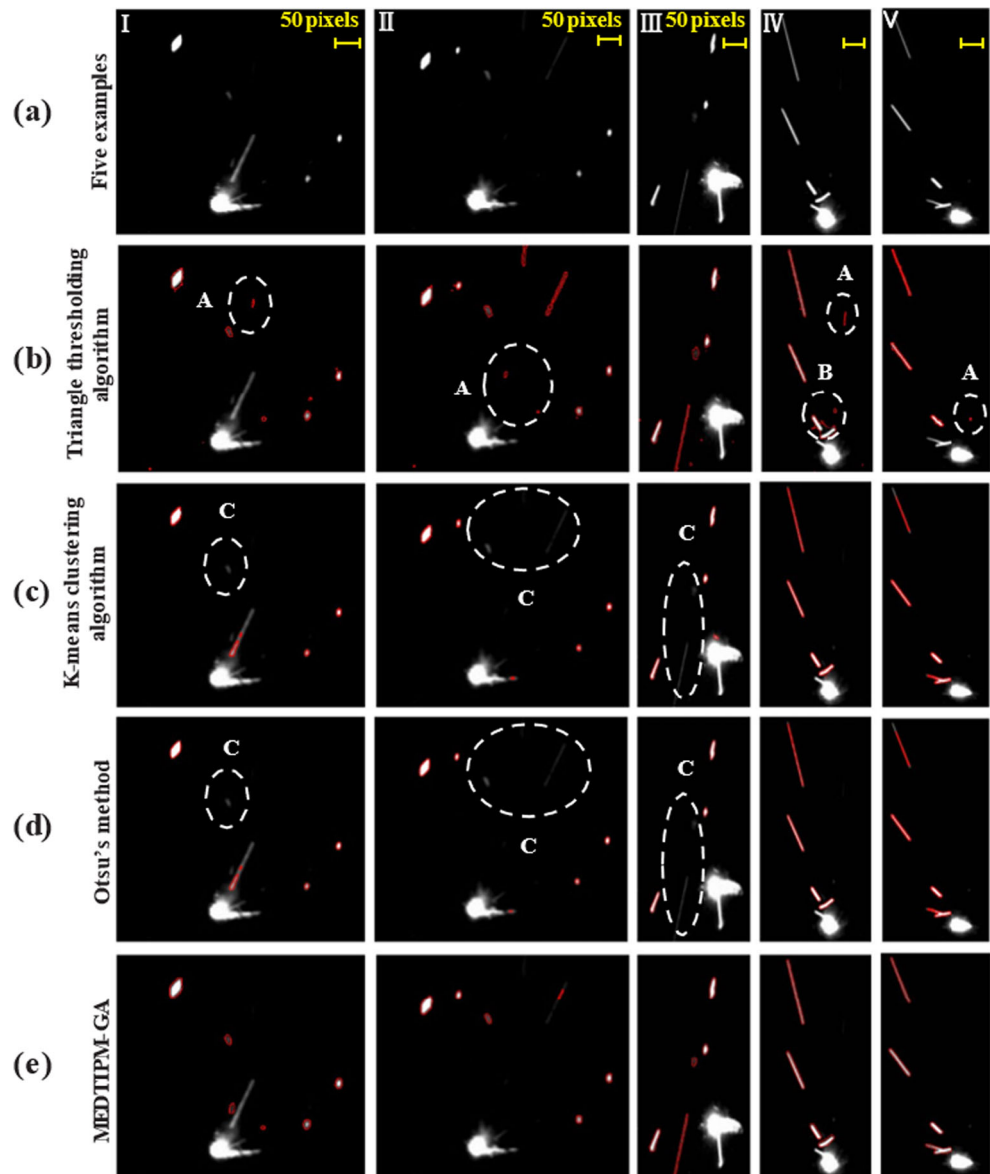


Fig. 18 Flowchart of the machine learning process implemented (reproduced from [55], Copyright (2018), with permission from Elsevier)



**Fig. 19** Formation mechanisms of spatter (reproduced from [58], Copyright (2016), with permission from Elsevier)

**Fig. 20** Comparison of image processing: **a** the target images, **b** triangle threshold segmentation algorithm, **c** K-means clustering algorithm, **d** Otsu's method, **e** MEDTIA-GA (the dashed white curves indicate the occurrence of errors) (reproduced from [60], Copyright (2020), with permission from Elsevier)



Kwon et al. [61] used a high-speed camera and field programmable gate array (FPGA) chip to form a molten pool image acquisition system and used a deep neural network framework to classify image data (refer to reference 61 for details of neural network). The classification failure rate of 13,200 test images using the deep neural network is less than 1.1%, and this model can be used to infer the location that caused the unexpected change in the microstructure. Velo3D has developed the VELO 3D Assure™ intelligent inspection system. The system first simulates the parts processing process, generates processing strategies, and then goes through various process controls to ensure the quality stability and consistency of multiple parts processing. The system can detect and mark process abnormalities and display corrective actions to avoid repeated errors. Differences can be reduced by real-time monitoring based on multiple sensors and machine algorithms.

## 6 Summary and prospect

Different behavior characteristics can be observed during the SLM forming process, including the existing research on molten pool signal, temperature signal, sound signal, scanning track, slice and powder layer, vibration of scraper system, deformation of parts and base plate, etc. Some scholars use a high-speed camera system, non-contact pyrometer, near-infrared thermal CMOS camera, photodiode, and microphone to collect the molding process signal. Acoustic emission technology and optical coherence tomography in situ non-destructive testing system may be applied to SLM molding monitoring. Data processing of monitored signals remains a huge challenge. The monitoring process produces high-frequency big data flow, which needs to use data infrastructures such as workstation, data storage, and analysis based on the network system and centralized server. The defect detection method based on deep learning is developed, and data mining and statistical analysis are used for effective data monitoring. The real-time processing of the monitored data requires high pixel and high sampling frequency, such as high sampling frequency of molten pool and track monitoring and high-speed camera system to capture the high pixel of melt change, which makes the real-time analysis challenging. The current research is still to confirm the feasibility of a monitoring method, but there is no relevant report on the research of corrective or feedback control measures.

There are still some obstacles in the robustness, stability, and repeatability of SLM. The trial-and-error method is still the mainstream research technology. The destructive method is used to test the performance of the specimen through the design of relevant experiments. In recent years, researchers have shifted their research from

molding technology to molding processes. The monitoring of molten pool, the tracking and planning of scanning path, the monitoring of plasma, the monitoring of acoustic signal in the forming process, and the temperature monitoring are mainly studied. The online monitoring technology for SLM process can monitor the forming quality online and in real time. The application of in situ monitoring technology can avoid destructive testing and high off-line detection costs. It can achieve the goal of intelligent and efficient forming by developing intelligent equipment that can adjust SLM parameters (including equipment parameters and process parameters) in real time.

The research hotspot of SLM field detection and closed-loop control technology is still in its infancy; many institutions are actively carrying out this research. Many developed systems can better understand the mechanism by monitoring the SLM forming process. Some coaxial monitoring systems have been embedded in commercial SLM equipment, but further research on feedback control strategy is needed to make full and efficient use of these monitoring systems. Scholars use the paraxial monitoring system to monitor the forming process because some SLM equipment do not have coaxial monitoring. Using paraxial monitoring usually requires higher magnification, higher measurable temperature range and higher acquisition rate. Machine vision and high-speed cameras are used to identify processing errors of SLM, such as powder bed conditions and geometric accuracy. However, the problems such as limited resolution, limited monitoring range (unable to track laser for monitoring), large amount of data brought by monitoring, and limited real-time data processing capacity of the computer need to be solved. To achieve effective closed-loop control, it is necessary to develop efficient sensors, improve the resolution of the monitoring machine, and use workstations and other equipment to improve the ability of the machine to analyze data. Few scholars put forward the control strategy of corrective or reactive actions after defects are detected. The SLM process is lack of robustness and stability, which is a major problem worthy of great research and technological progress. The development of in situ monitoring solution is the key to promote the industrialization of metal additive manufacturing.

**Acknowledgments** This work was supported by grants 51875010 and 51875005 from the National Natural Science Foundation of China. The authors gratefully acknowledge their financial support.

**Funding** This research was funded by the National Natural Science Foundation of China Grant Number 51875010 and 51875005.

## Compliance with ethical standards

**Conflict of interest** The authors declare that they have no conflict of interest.

## References

- Gunasekaran J, Sevvel P, John Solomon I (2020) Metallic materials fabrication by selective laser melting: a review. *Mater Today Proc*. <https://doi.org/10.1016/j.matpr.2020.05.162>
- Zhang C, Zhu J, Zheng H, Li H, Liu S, Cheng GJ (2020) A review on microstructures and properties of high entropy alloys manufactured by selective laser melting. *Int J Extreme Manuf* 2: 32003. <https://doi.org/10.1088/2631-7990/ab9ead>
- Craeghs T, Bechmann F, Berumen S, Kruth JP (2010) Feedback control of layerwise laser melting using optical sensors. *Phys Procedia* 5:505–514. <https://doi.org/10.1016/j.phpro.2010.08.078>
- Everton SK, Hirsch M, Stravroulakis P, Leach RK, Clare AT (2016) Review of in-situ process monitoring and in-situ metrology for metal additive manufacturing. *Mater Des* 95:431–445. <https://doi.org/10.1016/j.matdes.2016.01.099>
- Grasso M, Demir AG, Previtali B, Colosimo BM (2018) In situ monitoring of selective laser melting of zinc powder via infrared imaging of the process plume. *Robot Comput Integr Manuf* 49: 229–239. <https://doi.org/10.1016/j.rcim.2017.07.001>
- Gusarov AV, Smurov I (2009) Two-dimensional numerical modelling of radiation transfer in powder beds at selective laser melting. *Appl Surf Sci* 255:5595–5599. <https://doi.org/10.1016/j.apsusc.2008.07.202>
- Shiomi M, Osakada K, Nakamura K, Yamashita T, Abe F (2004) Residual stress within metallic model made by selective laser melting process. *CIRP Ann* 53:195–198. [https://doi.org/10.1016/S0007-8506\(07\)60677-5](https://doi.org/10.1016/S0007-8506(07)60677-5)
- Spears TG, Gold SA (2016) In-process sensing in selective laser melting (SLM) additive manufacturing. *Integr Mater Manuf Innov* 5:16–40. <https://doi.org/10.1186/s40192-016-0045-4>
- Van EM (2007) Complexity of selective laser melting: a new optimisation approach. Dissertation, Katholieke Universiteit Leuven. [https://lmo.libis.be/primoexplore/fulldisplay?docid=LIRIAS1746431&context=L&vid=Lirias&search\\_scope=Lirias&tab=default\\_tab&lang=en\\_US](https://lmo.libis.be/primoexplore/fulldisplay?docid=LIRIAS1746431&context=L&vid=Lirias&search_scope=Lirias&tab=default_tab&lang=en_US). Accessed 10 Oct 2020
- Thijs L, Verhaeghe F, Craeghs T, Humbeek JV, Kruth JP (2010) A study of the microstructural evolution during selective laser melting of Ti–6Al–4V. *Acta Mater* 58:3303–3312. <https://doi.org/10.1016/j.actamat.2010.02.004>
- Grasso M, Colosimo B (2017) Process defects and in-situ monitoring methods in metal powder bed fusion: a review. *Meas Sci Technol* 28:1–25. <https://doi.org/10.1088/1361-6501/aa5c4f>
- Yang J, Han J, Yu H, Yin JGM, Wang Z, Zeng X (2016) Role of molten pool mode on formability, microstructure and mechanical properties of selective laser melted Ti–6Al–4V alloy. *Mater Des* 110:558–570. <https://doi.org/10.1016/j.matdes.2016.08.036>
- Khairallah SA, Anderson AT, Rubenchik A, King WE (2016) Laser powder-bed fusion additive manufacturing: physics of complex melt flow and formation mechanisms of pores, spatter, and denudation zones. *Acta Mater* 108:36–45. <https://doi.org/10.1016/j.actamat.2016.02.014>
- Criales LE, Arsoy YM, Lane B, Moylan S, Donmez A, Özel T (2017) Laser powder bed fusion of nickel alloy 625: experimental investigations of effects of process parameters on melt pool size and shape with spatter analysis. *Int J Mach Tools Manuf*. 121:22–36. <https://doi.org/10.1016/j.ijmactools.2017.03.004>
- Foster B, Reutzel E, Nassar A, Hall B, Brown S, Dickman C (2015) 2015 Annual Solid Freeform Fabrication, Austin. In: University of Texas at Austin, pp 295–307. View Record in Scopus (<https://www.scopus.com/record/display.uri?eid=2-s2.0-84981188889&origin=inward&txid=9ac2b1abe9d6a36a40df1464e086c7b2>) Google Scholar ([https://scholar.google.com/scholar\\_lookup?title=Optical%2C%20layerwise%20monitoring%20of%20powder%20bed%20fusion&publication\\_year=2015&author=B.K.%20Foster&author=E.W.%20Reutzel&author=A.R.%20Nassar&author=B.T.%20Hall&author=S.W.%20Brown&author=C.J.%20Dickman](https://scholar.google.com/scholar_lookup?title=Optical%2C%20layerwise%20monitoring%20of%20powder%20bed%20fusion&publication_year=2015&author=B.K.%20Foster&author=E.W.%20Reutzel&author=A.R.%20Nassar&author=B.T.%20Hall&author=S.W.%20Brown&author=C.J.%20Dickman)). Accessed 10 Oct 2020
- Mani M, Donmez M, Feng S, Moylan S, Fesperman R, Lane B (2015) Measurement science needs for real-time control of additive manufacturing powder bed fusion processes. <https://doi.org/10.6028/NIST.IR.8036>
- Gibson BT, Bandari YK, Richardson BS, Henry WC, Vetland EJ, Sundermann TW, Love LJ (2020) Melt pool size control through multiple closed-loop modalities in laser-wire directed energy deposition of Ti–6Al–4V. *Addit Manuf* 32:100993. <https://doi.org/10.1016/j.addma.2019.100993>
- Gibson B, Bandari YK, Richardson B, Roschli A, Post B, Borish M, Thornton AS, Henry WC, Lamsey MD, Love L (2019) Melt pool monitoring for control and data analytics in large-scale metal additive manufacturing. United States. <https://www.osti.gov/biblio/1561633>. Accessed 10 Oct 2020
- Nassar AR, Reutzel EW, Brown SW Jr, John PM, Morgan JP, Natale DJ, Tutwiler RL, Feck DP, Banks JC (2016) Sensing for directed energy deposition and powder bed fusion additive manufacturing at Penn State University. In: *Proc.SPIE*. <https://doi.org/10.1117/12.2217855>
- Rodriguez E, Medina F, Espalin D, Terrazas C, Muse D, Henry C, Macdonald E, Wicker RB (2012) Integration of a thermal imaging feedback control system in electron beam melting. In: 23rd Annu Int Solid Free Fabr Symp - An Addit Manuf Conf SFF 2012, pp 945–961
- Chivel Y, Smurov I (2010) On-line temperature monitoring in selective laser sintering/melting. *Phys Procedia* 5:515–521. <https://doi.org/10.1016/j.phpro.2010.08.079>
- Pavlov M, Doubenskaia M, Smurov I (2010) Pyrometric analysis of thermal processes in SLM technology. *Phys Procedia* 5:523–531. <https://doi.org/10.1016/j.phpro.2010.08.080>
- Doubenskaia M, Pavlov M, Chivel Y (2010) Optical system for on-line monitoring and temperature control in selective laser melting technology. *Key Eng Mater* 437:458–461. <https://doi.org/10.4028/www.scientific.net/KEM.437.458>
- Doubenskaia M, Pavlov M, Grigoriev S, Tikhonova E, Smurov I (2012) Comprehensive optical monitoring of selective laser melting. *J Laser Micro / Nanoeng* 7:236–243. <https://doi.org/10.2961/jlmn.2012.03.001>
- Berumen S, Bechmann F, Lindner S, Kruth JP, Tom C (2010) Quality control of laser-and powder bed-based additive manufacturing (AM) technologies. *Phys Procedia* 5:617–622. <https://doi.org/10.1016/j.phpro.2010.08.089>
- Clijsters S, Craeghs T, Buls S, Kempen K, Kruth JP (2014) In situ quality control of the selective laser melting process using a high-speed, real-time melt pool monitoring system. *Int J Adv Manuf Technol* 75:1089–1101. <https://doi.org/10.1007/s00170-014-6214-8>
- Craeghs T, Clijsters S, Yasa E, Bechmann F, Berumen S, Kruth JP (2011) Determination of geometrical factors in layerwise laser melting using optical process monitoring. *Opt Lasers Eng* 49: 1440–1446. <https://doi.org/10.1016/j.optlaseng.2011.06.016>
- Craeghs T, Clijsters S, Kruth JP, Bechmann F, Ebert MC (2012) Detection of process failures in layerwise laser melting with optical process monitoring. *Phys Procedia* 39:753–759. <https://doi.org/10.1016/j.phpro.2012.10.097>
- Yadroitsev I, Krakhmalev P, Yadroitsava I (2014) Selective laser melting of Ti6Al4V alloy for biomedical applications: temperature monitoring and microstructural evolution. *J Alloys Compd* 583: 404–409. <https://doi.org/10.1016/j.jallcom.2013.08.183>
- Lott P, Schleifenbaum H, Meiners W, Wissenbach K, Hinke C, Bültmann J (2011) Design of an optical system for the in situ process monitoring of selective laser melting (SLM). *Phys Procedia* 12: 683–690. <https://doi.org/10.1016/j.phpro.2011.03.085>



31. Thombansen U, Gatej A, Pereira M (2014) Process observation in fiber laser-based selective laser melting. *Opt Eng* 54:11008. <https://doi.org/10.1117/1.OE.54.1.011008>
32. Fercher AF, Drexler W, Hitzinger CK, Lasser T (2003) Optical coherence tomography - principles and applications. *Rep Prog Phys* 66:239–303. <https://doi.org/10.1088/0034-4885/66/2/204>
33. Kanko JA, Sibley AP, Fraser JM (2016) In situ morphology-based defect detection of selective laser melting through inline coherent imaging. *J Mater Process Technol* 231:488–500. <https://doi.org/10.1016/j.jmatprotec.2015.12.024>
34. Neef A, Seyda V, Herzog D, Emmelmann C, Schönleber M, Kogel-Hollacher M (2014) Low coherence interferometry in selective laser melting. *Phys Procedia* 56:82–89. <https://doi.org/10.1016/j.phpro.2014.08.100>
35. Krauss H, Eschey C, Zaeh MF (2012) Thermography for monitoring the selective laser melting process. In: 23rd International Solid Freeform Fabrication Symposium; Austin, TX. <https://api.semanticscholar.org/CorpusID:201858857>. Accessed 10 Oct 2020. Google Scholar ([https://scholar.google.com/scholar\\_lookup?title=Thermography%20for%20monitoring%20the%20selective%20laser%20melting%20process&publication\\_year=2012&author=H.%20Krauss&author=C.%20Eschey&author=M.F.%20Zaeh](https://scholar.google.com/scholar_lookup?title=Thermography%20for%20monitoring%20the%20selective%20laser%20melting%20process&publication_year=2012&author=H.%20Krauss&author=C.%20Eschey&author=M.F.%20Zaeh))
36. Kleszczynski S, Zur Jacobsmühlen J, Seht JT, Witt G (2012) Error detection in laser beam melting systems by high resolution imaging. In: 23rd Annu. Int. Solid Free. Fabr. Symp. University of Texas at Austin, Austin, pp 975–987. Google Scholar ([https://scholar.google.com/scholar?hl=zh-CN&as\\_sdt=2005&sciodt=0%2C5&cites=3082008579271783940&scipsc=&q=Error+detection+in+laser+beam+melting+systems+by+high+resolution+imaging&btnG=](https://scholar.google.com/scholar?hl=zh-CN&as_sdt=2005&sciodt=0%2C5&cites=3082008579271783940&scipsc=&q=Error+detection+in+laser+beam+melting+systems+by+high+resolution+imaging&btnG=))
37. Jacobsmühlen JZ, Kleszczynski S, Schneider D, Witt G (2013) High resolution imaging for inspection of laser beam melting systems. In: 2013 IEEE international instrumentation and measurement technology conference (I2MTC), 6–9 May 2013 (pp 707–712). <https://doi.org/10.1109/I2MTC.2013.6555507>. Google Scholar ([https://hk7096.scholar.eu.org/scholar?hl=zh-CN&as\\_sdt=0%2C5&q=High+resolution+imaging+for+inspection+of+laser+beam+melting+systems&btnG=](https://hk7096.scholar.eu.org/scholar?hl=zh-CN&as_sdt=0%2C5&q=High+resolution+imaging+for+inspection+of+laser+beam+melting+systems&btnG=))
38. Jacobsmühlen JZ, Kleszczynski S, Witt G, Merhof D (2015) Elevated region area measurement for quantitative analysis of laser beam melting process stability. In: 26th International solid freeform fabrication symposium, Austin, TX. Google Scholar ([https://xueshu.lanfanshu.cn/scholar?hl=zh-CN&as\\_sdt=2005&sciodt=0%2C5&scipsc=&q=Elevated+Region+Area+Measurement+for+Quantitative+Analysis+of+Laser+Beam+Melting+Process+for+Stability&btnG=](https://xueshu.lanfanshu.cn/scholar?hl=zh-CN&as_sdt=2005&sciodt=0%2C5&scipsc=&q=Elevated+Region+Area+Measurement+for+Quantitative+Analysis+of+Laser+Beam+Melting+Process+for+Stability&btnG=))
39. Jacobsmühlen JZ, Kleszczynski S, Witt G, Merhof D (2015) Detection of elevated regions in surface images from laser beam melting processes. In: 41st Annual conference of the IEEE Industrial Electronics Society. Google Scholar ([https://hk7096.scholar.eu.org/scholar?hl=zh-CN&as\\_sdt=0%2C5&q=Detection+of+elevated+regions+in+surface+images+from+laser+beam+melting+processes&btnG=](https://hk7096.scholar.eu.org/scholar?hl=zh-CN&as_sdt=0%2C5&q=Detection+of+elevated+regions+in+surface+images+from+laser+beam+melting+processes&btnG=))
40. Hirvimäki M, Manninen M, Lehti A, Happonen A, Salminen A, Nyrhilä O (2013) Evaluation of different monitoring methods of laser additive manufacturing of stainless steel. *Adv Mater Res* 651:812–819. <https://doi.org/10.4028/www.scientific.net/AMR.651.812>
41. Zhao C, Fezzaa K, Cunningham RW, Wen H, Carlo FD, Chen L, Rollett AD, Sun T (2017) Real-time monitoring of laser powder bed fusion process using high-speed X-ray imaging and diffraction. *Sci Rep* 7:1–11. <https://doi.org/10.1038/s41598-017-03761-2>
42. Craeghs T, Clijsters S, Yasa E, Kruth J-P (2011) Online quality control of selective laser melting. In: 22nd Annu. Int. Solid Free. Fabr. Symp. - An Addit. Manuf. Conf. SFF 2011. University of Texas at Austin (freeform), Austin, pp 212–226. Google Scholar ([https://xueshu.lanfanshu.cn/scholar?hl=zh-CN&as\\_sdt=2005&sciodt=0%2C5&scipsc=&q=Online+quality+control+of+selective+laser+melting&btnG=](https://xueshu.lanfanshu.cn/scholar?hl=zh-CN&as_sdt=2005&sciodt=0%2C5&scipsc=&q=Online+quality+control+of+selective+laser+melting&btnG=)). Accessed 10 Oct 2020
43. Bayle F, Doubenskaia M (2008) Selective laser melting process monitoring with high speed infra-red camera and pyrometer - art. no. 698505. In: *Proc SPIE*, vol 6985. <https://doi.org/10.1117/12.786940>
44. Repposini G, Laguzza V, Grasso M, Colosimo BM (2017) On the use of spatter signature for in-situ monitoring of laser powder bed fusion. *Addit Manuf* 16:35–48. <https://doi.org/10.1016/j.addma.2017.05.004>
45. Furumoto T, Alkahari MR, Ueda T, Aziz MSA, Hosokawa A (2012) Monitoring of laser consolidation process of metal powder with high speed video camera. *Phys Procedia* 39:760–766. <https://doi.org/10.1016/j.phpro.2012.10.098>
46. Islam M, Purtonen T, Piili H, Salminen A, Nyrhilä O (2013) Temperature profile and imaging analysis of laser additive manufacturing of stainless steel. *Phys Procedia* 41:835–842. <https://doi.org/10.1016/j.phpro.2013.03.156>
47. Kruth JP, Froyen L, Van Vaerenbergh J, Mercelis P, Rombouts M, Lauwers B (2004) Selective laser melting of iron-based powder. *J Mater Process Technol* 149:616–622. <https://doi.org/10.1016/j.jmatprotec.2003.11.051>
48. Krauss H, Zeugner T, Zaeh MF (2014) Layerwise monitoring of the selective laser melting process by thermography. *Phys Procedia* 56:64–71. <https://doi.org/10.1016/j.phpro.2014.08.097>
49. Krauss H, Zeugner T, Zaeh M (2015) Thermographic process monitoring in powderbed based additive manufacturing. *AIP Conf Proc* 1650:177–183. <https://doi.org/10.1063/1.4914608>
50. Abdelrahman M, Reutzel EW, Nassar AR, Starr TL (2017) Flaw detection in powder bed fusion using optical imaging. *Addit Manuf* 15:1–11. <https://doi.org/10.1016/j.addma.2017.02.001>
51. Ye DS, Hong GS, Zhang YJ, Zhu KP, Fuh JYH (2018) Defect detection in selective laser melting technology by acoustic signals with deep belief networks. *Int J Adv Manuf Technol* 96:2791–2801. <https://doi.org/10.1007/s00170-018-1728-0>
52. Leung CLA, Marussi S, Atwood RC, Towrie M, Withers PJ, Lee PD (2018) In situ X-ray imaging of defect and molten pool dynamics in laser additive manufacturing. *Nat Commun* 9:1355. <https://doi.org/10.1038/s41467-018-03734-7>
53. Boaretto N, Centeno TM (2017) Automated detection of welding defects in pipelines from radiographic images DWDI. *NDT E Int* 86:7–13. <https://doi.org/10.1016/j.ndteint.2016.11.003>
54. Yuan B, Giera B, Guss G, Matthews M, McMains S, (2019) Semi-supervised convolutional neural networks for in-situ video monitoring of selective laser melting. 2019 IEEE Winter Conference on Applications of Computer Vision (WACV). IEEE, 2019. <https://doi.org/10.1109/WACV.2019.00084>
55. Scime L, Beuth J (2018) Anomaly detection and classification in a laser powder bed additive manufacturing process using a trained computer vision algorithm. *Addit Manuf* 19:114–126. <https://doi.org/10.1016/j.addma.2017.11.009>
56. Scime L, Beuth J (2018) A multi-scale convolutional neural network for autonomous anomaly detection and classification in a laser powder bed fusion additive manufacturing process. *Addit Manuf* 24:273–286. <https://doi.org/10.1016/j.addma.2018.09.034>
57. Hoffman J, Szymanski Z (2004) Time-dependent spectroscopy of plasma plume under laser welding conditions. *J Phys D Appl Phys* 37:1792–1799. <https://doi.org/10.1088/0022-3727/37/13/010>
58. Wang D, Wu S, Fu F, Mai S, Yang Y, Liu Y, Song C (2017) Mechanisms and characteristics of spatter generation in SLM processing and its effect on the properties. *Mater Des* 117:121–130. <https://doi.org/10.1016/j.matdes.2016.12.060>
59. Grasso M, Colosimo BM (2019) A statistical learning method for image-based monitoring of the plume signature in laser powder bed

- fusion. *Robot Comput Integr Manuf* 57:103–115. <https://doi.org/10.1016/j.rcim.2018.11.007>
60. Yang D, Li H, Liu S, Song C, Yang Y, Shen S, Lu J, Liu Z, Zhu Y (2020) In situ capture of spatter signature of SLM process using maximum entropy double threshold image processing method based on genetic algorithm. *Opt Laser Technol* 131:106371. <https://doi.org/10.1016/j.optlastec.2020.106371>
61. Kwon O, Kim HG, Ham MJ, Kim W, Kim GH, Cho JH, Kim NI, Kim K (2020) A deep neural network for classification of melt-pool images in metal additive manufacturing. *J Intell Manuf* 31:375–386. <https://doi.org/10.1007/s10845-018-1451-6>

**Publisher's note** Springer Nature remains neutral with regard to jurisdictional claims in published maps and institutional affiliations.